JOURNAL OF PETROLOGY | VOLUME 43 | NUMBER 3 | PAGES 557–577 | 2002

U–Th Disequilibrium and Rb–Sr Age Constraints on the Magmatic Evolution of Peralkaline Rhyolites from Kenya

ARND HEUMANN[1,2]* AND GARETH R. DAVIES[1]

[1]FACULTEIT DER AARDWETENSCHAPPEN, VRIJE UNIVERSITEIT AMSTERDAM, DE BOELELAAN 1085, 1081 HV AMSTERDAM, THE NETHERLANDS

[2]GEOCHEMISCHES INSTITUT, GEORG-AUGUST-UNIVERSITÄT, GOLDSCHMIDTSTR. 1, 37077 GÖTTINGEN, GERMANY

RECEIVED AUGUST 10, 2000; REVISED TYPESCRIPT ACCEPTED SEPTEMBER 25, 2001

Mildly peralkaline rhyolites of the Olkaria Volcanic Complex, located in the Kenyan sector of the East African rift valley, have low Sr concentrations and elevated Rb/Sr ratios (Sr 1·3–2 ppm; $^{87}Rb/^{86}Sr$ = 748–1769) that potentially allow the resolution of time differences on the order of 1 ka by conventional Sr isotope determination. Because of their young eruption ages (≤ 20 ka), a chemically independent assessment of the Sr isotope results has been obtained by U-series dating. Rb–Sr isochron ages of pristine glasses and phenocrysts from the most chemically evolved rhyolites pre-date the eruption ages and are best defined by a mineral isochron of 24 ± 1 ka. The glasses are in secular U–Th equilibrium so that no age information can be obtained. In contrast, glasses and minerals yield U–Th isochrons of 25 ± 10 ka and are probably controlled by the Th-enriched accessory phase chevkinite. We therefore ascribe the pre-eruptive age information to crystallization of the observed phenocryst phases. Inferred high magma fractionation rates of up to 2·5 × 10^{-3} km^3/yr are comparable with those for much larger metaluminous silicic magma systems. Magma storage times (~ 22 ky), however, are much shorter and may best be accounted for by the specific size, longevity and thermal gradient of the silicic magma system.

KEY WORDS: *silicic magmatism; isotope geochemistry; time scales; fractional crystallization; magma chambers; residence times*

INTRODUCTION

The aim of this study is to obtain absolute age information on magmatic processes occurring in a volumetrically minor, continental magma system of mildly peralkaline composition [molar $(Na_2O + K_2O)/Al_2O_3$ or agpaitic index, AI >1)]. The work was undertaken as a contrast to far larger, prominent, caldera-forming peralkaline (e.g. Mahood, 1984) or metaluminous volcanic systems such as Long Valley (e.g. Halliday *et al.*, 1989; Davies *et al.*, 1994). The goal is to assess how the rates of magmatic processes vary with the size or composition of the system. We utilize both the Rb–Sr and U–Th geochronometers because they have distinct chemical behaviour and respond in different ways to magmatic processes. Comparison of the two isotope systems therefore may provide additional insights into the time scales of processes that control the evolution of strongly differentiated silicic magmas.

Peralkaline felsic magmas are most widespread in regions of continental upwelling and/or rifting (Fitton & Upton, 1987), but actually occur in a wide variety of geodynamic settings, including oceanic islands (Caroff *et al.*, 1993; Mungall & Martin, 1995), island arcs (Bevier *et al.*, 1979) and extensional continental areas (Mahood, 1981; Civetta *et al.*, 1984; Macdonald, 1987). There are various petrogenetic explanations for the generation of peralkaline felsic magmas. Proposed models include derivation from the often closely associated alkali basaltic or mugearitic magmas by fractional crystallization (Nelson & Hegre, 1990; Mungall & Martin, 1995; Bohrson & Reid, 1998; Civetta *et al.*, 1998), partial melting of lower-crustal gabbroic cumulates (Lowenstern & Mahood, 1991) and partial melting of heterogeneous source regions, including

*Corresponding author. Present address: Faculteit der Aardwetenschappen, Vrije Universiteit Amsterdam, De Boelelaan 1085, 1081 HV Amsterdam, The Netherlands. Telephone: +31-20-44-47279. Fax: +31-20-646-2457. E-mail: heua@geo.vu.nl

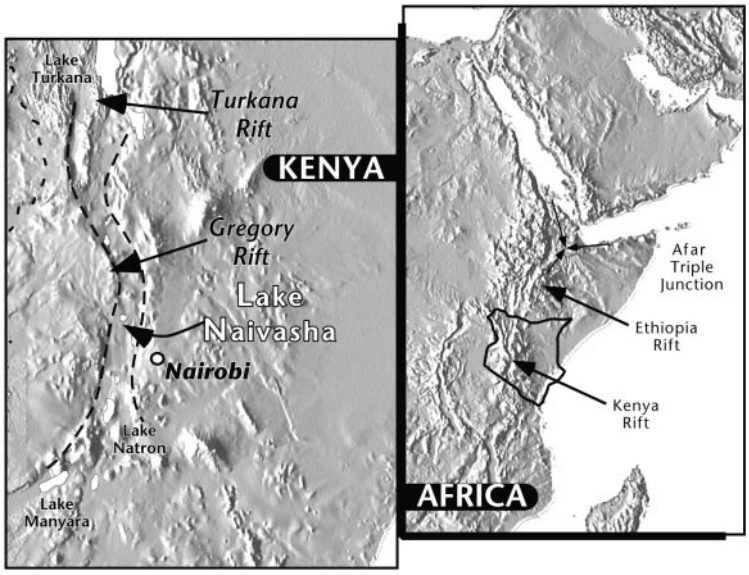

Fig. 1. Location of the Kenya Rift relative to the East African rift system.

metasomatized subcontinental mantle (Bailey & Macdonald, 1987) and upper-crustal lithologies (Davies & Macdonald, 1987; Macdonald *et al.*, 1987; Black *et al.*, 1997).

The Cenozoic volcanism associated with the East African rift system has produced enormous volumes of peralkaline volcanic rocks, some related to large caldera volcanoes generally younger than 1 Ma (Williams & Macdonald, 1984; Macdonald, 1987). Amongst the Quaternary volcanic rocks of the Kenya Rift Valley, the comenditic (mildly peralkaline) high-silica rhyolites of the Greater Olkaria Volcanic Complex (Clarke *et al.*, 1990), formerly termed the Naivasha complex (Macdonald *et al.*, 1987), are well suited for a study that assesses the rate at which magmatic processes occur. A comparative Rb–Sr and U–Th isotope investigation is possible because of their advanced degree of chemical differentiation, young eruption ages (20 ka–Recent) and glassy nature that allows determination of melt compositions.

GEOLOGICAL BACKGROUND

The Kenya Rift forms part of the eastern arm of the East African rift system and extends for nearly 1000 km from northern Tanzania to the Turkana basin (Fig. 1). Comprehensive reviews of the temporal, structural and magmatic evolution of the rift zone and its morphotectonic features have been presented by Smith & Mosley (1993), Macdonald *et al.* (1994*a*) and Smith (1994).

The focus of late Quaternary volcanism along the central part of the Kenya Rift coincides with a zone of crustal upwarping commonly termed the Kenya Dome (Macdonald *et al.*, 1994*b*; Smith, 1994). The Greater Olkaria Volcanic Complex (Fig. 2) lies close to the centre of this zone, near the large trachytic caldera volcanoes Longonot and Suswa and the pantelleritic (strongly peralkaline) complex Eburru (Macdonald, 1987; Clarke *et al.*, 1990). The Greater Olkaria Volcanic Complex comprises a volcanic dome and lava field (20 ka–Recent) of $\sim$250 km^2, comprising at least 80 small eruptive centres (Fig. 3). The dominantly comenditic lavas overlie basaltic, trachytic and rhyolitic lavas and pyroclastic deposits, at least 2·6 km thick, the top 1 km of which probably formed within the last 450 ky (Clarke *et al.*, 1990). Recent trachyte and basalt–hawaiite lavas, although volumetrically minor, occur marginally to, and partly commingled with, the comendites, indicating a complex plumbing system (Bone, 1987).

The aphyric to sparsely porphyritic Olkaria comendites [molar $(Na_2O + K_2O)/Al_2O_3 = 1{\cdot}0–1{\cdot}4$] are exceedingly halogen rich (F <0·95 wt %; Cl <0·47 wt %) and reveal highly fractionated melt compositions with strong trace element depletions (e.g. Ba, Sr) and enrichments (e.g. Rb, Th, Nb, Ta, Zr, REE) (Table 1). Subtle variations in light rare earth element/heavy rare earth element (LREE/HREE) or Zr/Nb ratios between eruptive centres, some contemporaneous, have been used to define seven chemostratigraphic groups (Macdonald *et al.*, 1987), which also appear to have distinct Sr–Nd–Pb isotope compositions (Davies & Macdonald, 1987). Consequently, Macdonald and coworkers interpreted the petrogenetic origin of the comendites to reflect discrete partial melting events of isotopically heterogeneous crustal source rocks promoted by influx of halogens (see Bailey & Macdonald, 1975, 1987). Similar conclusions

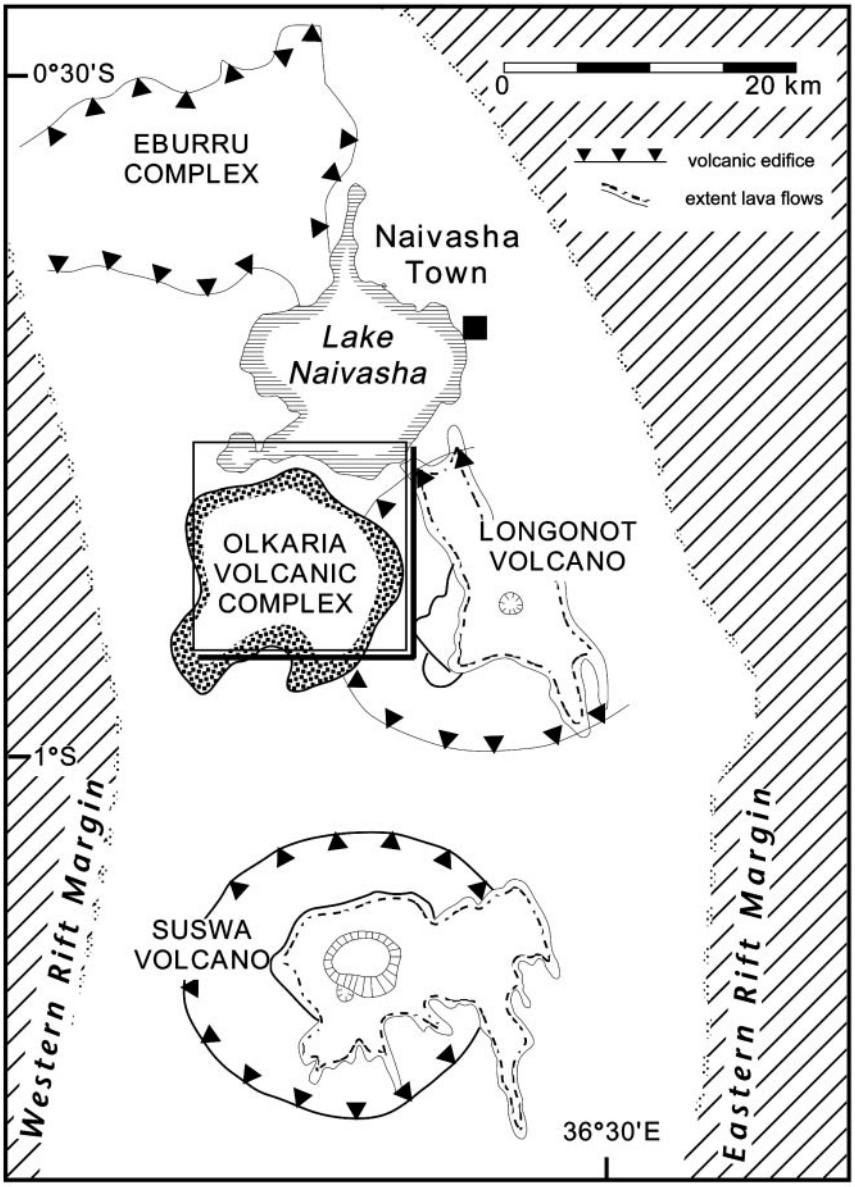

Fig. 2. Section of the East African rift valley near Lake Naivasha in Kenya showing the location of the Olkaria Volcanic Complex and the main volcano-structural features [after Clarke *et al.* (1990)].

have been drawn from a U-series disequilibrium study of the comendites (Black *et al.*, 1997).

A recent volcanological study interpreted the stratigraphy of the Olkaria comendites as a post-caldera dome-building phase following a long eruptive history documented in the underlying lithologies (Clarke *et al.*, 1990). According to this model, initiation of the recent comendite eruptions at $\sim$20 ka followed the deposition of a welded pantelleritic deposit. The Olkaria comendites were stratigraphically divided into a Lower, Middle and Upper Member and the most recent Ololbutot comendites. The use of the term 'caldera', however, may be misleading as the existence of such a structure is poorly constrained and, on the basis of the study by Clarke *et al.* (1990), the curved alignment of ring fracture domes is thought to delimit only 30% of a caldera rim. Nevertheless, chemical analyses (Clarke *et al.*, 1990) appear to support the broad division of products into four stratigraphic groups of comendites.

The Olkaria comendites are intercalated with pyroclastic fall deposits of the nearby trachytic Longonot volcano. ^{14}C dates of these Longonot successions obtained from palaeosoil horizons and wood (Clarke *et al.*, 1990) allow constraints to be placed on the eruption ages

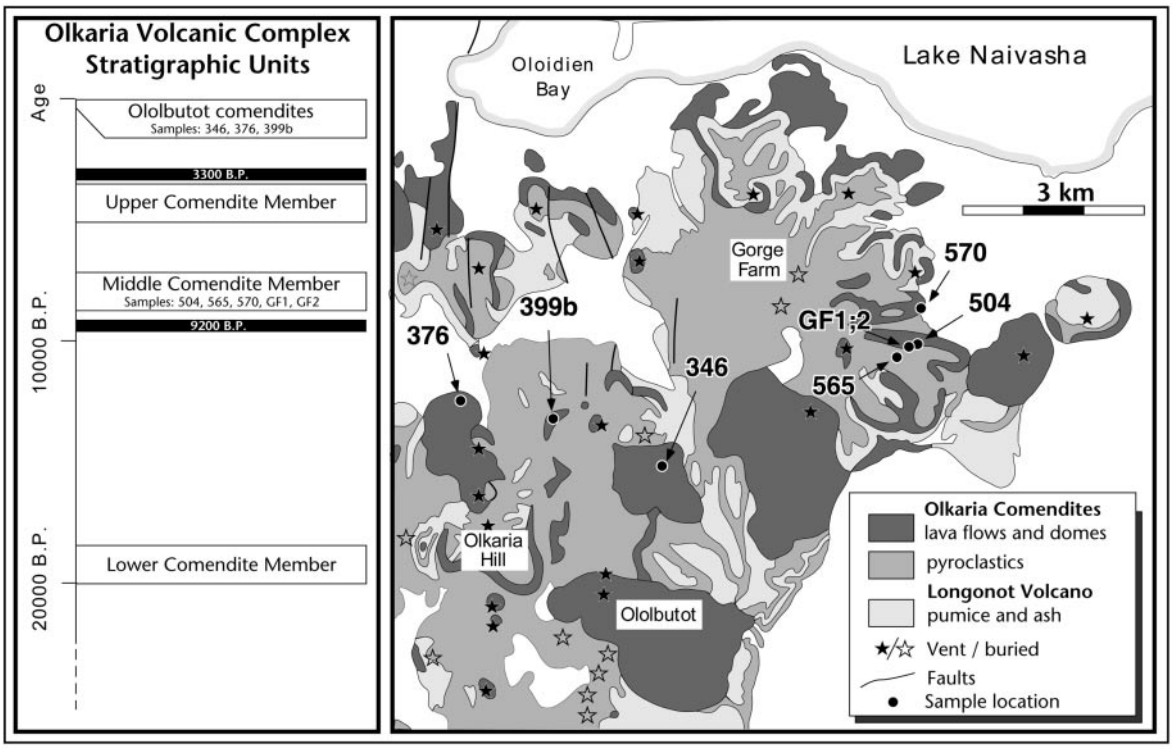

Fig. 3. Geological map showing sample locations from the Gorge Farm and Ololbutot–Olkaria centres of the Olkaria Volcanic Complex [redrawn from Clarke *et al.* (1990)].

of the various comendite groups. In agreement with stratigraphic relationships, the age of the Lower Comendite Member is ~20 ka, the Middle Member ~8 ka, and the Upper Member ~6 ka, which includes historic comendites at <200 yr.

SAMPLES

Samples used in this study are from the most evolved comendites of Groups 3 and 6 [following Macdonald *et al.* (1987)] and correspond to the Middle Comendite Member (~8 ka) and the most recent Ololbutot comendites (Clarke *et al.*, 1990). In detail, there are five samples from the Gorge Farm eruptive centre (Group 3) and three from the Olkaria Hill–Ololbutot fissure eruption centre (Group 6; Fig. 3). Sample locations and designations are identical to those of Macdonald *et al.* (1987) except for the additional GF samples. Figure 4 shows that comendites from those two locations have the most fractionated trace element characteristics in terms of Nb–Zr contents.

Gorge Farm (Fig. 3) is the largest eruptive centre of the Olkaria complex and lava flows represent a volume of ~5 km^3 [deduced from the geological map of Clarke *et al.* (1990)]. The Gorge Farm lavas are petrographically different from the other groups in that, in addition to the generally aphyric to sparsely porphyritic varieties of obsidians, there are also glassy lavas with 5–10% of phenocrysts. The samples used in this study have similar phenocryst assemblages of sanidine, quartz, biotite, amphibole, Fe–Ti oxides, and fayalite. Sample 570 contains additionally aenigmatite (Macdonald *et al.*, 1987). The chemical characteristics of the Gorge Farm lavas also distinguish them from other eruptive centres of comparable age. Although their SiO_2 contents, between 74 and 75 wt % (volatile-free), are lower than the general high-silica compositions of the Olkaria comendites, the degree of trace element enrichment is extreme (Table 1). Most notable are low Ba (1–3 ppm) and Sr (~1 ppm), and exceedingly high Th (110–120 ppm), U (22–25 ppm), Rb (590–640 ppm) and Ta (44–50 ppm) concentrations. Samples were taken on the northeastern slopes of the dome (Fig. 3).

The lavas of the Ololbutot centre were erupted from a north–south-aligned fissure structure of ~4 km length, located SW of the Gorge Farm centre (Fig. 3). Together with the lavas from the neighbouring Olkaria Hill, they belong to the most recent eruptive activity at the Olkaria complex. The sampled Ololbutot rocks vary from aphyric to phenocryst-poor obsidians (on average <2 vol. % phenocrysts), containing only minor amounts of quartz

Table 1: Whole-rock analyses of comendites used in this study [data from Macdonald et al. (1987)]

	Gorge Farm centre (Group 3; age ≤8 ka)			Ololbutot centre (Group 6; age ≤1 ka)		
Sample:	504	565	570	346	376	399b
SiO_2	72·9	72·5	73·1	73·0	73·5	73·3
TiO_2	0·23	0·24	0·33	0·29	0·22	0·22
Al_2O_3	10·44	10·32	10·52	10·32	10·23	10·45
Fe_2O_3	1·90	1·93	1·93	1·89	1·87	1·61
FeO	2·21	2·25	2·15	2·30	2·27	2·01
MnO	0·06	0·06	0·04	0·06	0·05	0·04
MgO	0·02	0·02	0·02	0·01	0·02	0·01
CaO	0·15	0·15	0·13	0·21	0·18	0·19
Na_2O	5·54	5·86	5·74	5·90	5·95	5·56
K_2O	4·36	4·39	4·45	4·41	4·41	4·45
P_2O_5				0·02		0·01
H_2O^+	0·27	0·23	0·13	0·03	0·03	0·60
H_2O^-	0·07	0·03	0·09	0·19	0·20	0·13
F	0·90	0·95	0·91	0·82	0·67	0·62
Cl	0·47	0·47	0·44	0·37	0·38	0·32
O = F,Cl	0·49	0·51	0·48	0·43	0·37	0·33
Total	99·03	98·89	99·50	99·39	99·61	99·19
Ba	2	3	1	3	3	1
Cs	10·9	12	10·9	8·4	8·9	6·5
Hf	55·3	60·5	54·1	52·1	53·2	40·9
Nb	541	590	531	446	457	357
Pb	62	68	62	60	62	52
Rb	602	637	593	471	486	403
Sc	0·33	0·3	0·32	0·16	0·17	0·13
Sr		1·253	1·586		2·029	1·513
Ta	44	49·4	43·9	34	34·9	26·1
Th	111	124	108	88·6	90·6	66·9
U	22·5	25·1	22·9	16·1	17·1	13·6
Y	276	296	275	258	259	222
Zr	1882	2018	1832	1892	1909	1577
La	145	153	140	169	172	129
Ce	300	310	288	345	348	259
Nd	120	151	116	145	144	107
Sm	33·8	36·8	33·1	34·3	35·4	24·2
Eu	0·45	0·47	0·43	0·66	0·72	0·56
Gd	38·4	42·2	36·9	39·1	37·8	31·8
Yb	30·0	34·6	31·4	26·8	27·6	22·0
Lu	4·03	4·33	3·86	3·68	3·73	2·86

See Macdonald *et al.* (1987) for details of petrography.

and sanidine and apparently no mafic phases. Compared with the Gorge Farm samples, the Ololbutot lavas show less extreme depletion or enrichment in trace elements, e.g. Sr (~2 ppm), Rb (400–490 ppm), Th (67–90 ppm), U (13–17 ppm) and Ta (26–35 ppm). Major element compositions and AI values (1·3–1·4) for samples from

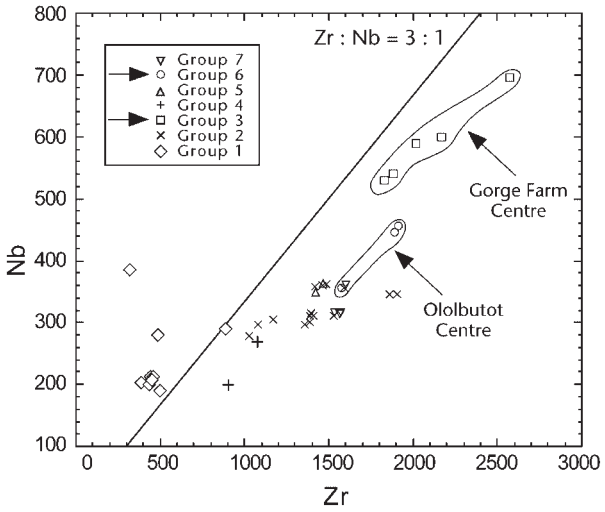

Fig. 4. Nb vs Zr diagram of Olkaria comendites following the classification into seven chemostratigraphic groups (Macdonald *et al.*, 1987) with Group 3 and 6 rocks showing the most fractionated compositions.

the two locations are, however, indistinguishable, apart from F and Cl concentrations (Macdonald *et al.*, 1987).

ANALYTICAL TECHNIQUES

To further investigate the unusual trace element characteristics of the Olkaria rocks, notably the Sr depletion and enrichments in Rb, U and Th, the O, Ar, Nd, Pb, Rb–Sr and U–Th isotope systematics were determined on glasses and minerals. After critical inspections for impurities, especially mineral inclusions, about 200 mg of glass and 30–200 mg of sanidine, biotite, amphibole, fayalite, magnetite and quartz (~5 g) were carefully hand picked from a 200–400 μm grain-size fraction. Separates were repeatedly cleaned and then dissolved in HF–HNO_3–$HClO_4$ mixtures. To include further mafic minerals that usually occur only in trace amounts (possibly aenigmatite and ilmenite), bulk magnetic mineral fractions of high density (D >3·0) were also included for analysis. For Pb isotope analyses of small sanidine fractions (2–4 grains), a separate chemical procedure was employed involving only 10% of the commonly used amounts of acids. The total procedural blanks for Pb, Sr, Nd, U and Th were <150, <250, <50, <30 and 13 pg, respectively. The isotopic compositions of Pb and Sr were measured by thermal-ionization mass spectrometry (TIMS) on a Finnigan MAT 261 system, and Nd, U and Th on a MAT 262 RPQ_{Plus} system, following the techniques outlined by Heumann & Davies (1997). Concentrations of Rb, Sr, Th and U were obtained by isotope dilution. The mean values for NBS 987 were $^{87}Sr/^{86}Sr$ = 0·710270 ± 15 (n = 11) and for an internal Nd-standard $^{143}Nd/^{144}Nd$ = 0·51135 ± 15 (n = 25). Corrections for mass-fractionation are based on $^{86}Sr/^{88}Sr$ = 0·1194, $^{146}Nd/^{144}Nd$ = 0·7219 and a discrimination factor of 0·113% per a.m.u. for Pb obtained from multiple measurements of NBS 981. Details of U–Th standard measurements and reproducibilities are identical to those described by Heumann (1999) and Fruijtier *et al.* (2000). Accuracy was verified by repeated measurements of the TML rock standard, for which we measured secular equilibrium ($^{238}U/^{232}Th$ = 1·081 and $^{230}Th/^{238}U$ = 1·000). Additional details will be given elsewhere (Heumann *et al.*, 2002). All isochron ages and their 2σ errors were calculated following standard least-squares fitting methods (McIntyre *et al.*, 1966; York, 1969; Titterington & Halliday, 1979).

^{40}Ar–^{39}Ar ages were determined to verify the very young eruption ages of the sampled comendite flows. For this purpose, irradiated bulk sanidine separates of two samples from each chemical group were split into four respective sets of 10–15 grains. Each set was individually fused and the released gas fraction analysed on the argon laser-probe in Amsterdam (Heumann, 1999). However, no age information could be deduced from the results, which confirmed that eruption ages are below the age resolution of the Ar–Ar technique (~10 ka).

Oxygen isotope compositions of glasses were measured by KrF laser-ablation mass spectrometry at the Geochemisches Institut in Göttingen, following the basic procedure of Wiechert & Hoefs (1995) but with a smaller sample chamber (Fiebig *et al.*, 1999). In the present study, the extracted oxygen was frozen on a 0·5 nm mol sieve and introduced into a gas-chromatograph, and isotopic ratios were analysed in a Delta-Plus mass spectrometer.

RESULTS

Rb–Sr isotopic compositions

The Rb/Sr ratios of glasses from the two eruptive centres are distinctly different (Table 2) and range between 258–294 (Ololbutot centre) and 510–611 (Gorge Farm centre). These values correspond to an overall variation of $^{87}Rb/^{86}Sr$ from 747 to 1769. The distinction between the centres is caused by very low Sr contents that are nearly constant in each group (2·0 and 1·3 ppm, respectively), whereas variable Rb concentrations (517–814 ppm) produce the within-group spread in Rb/Sr ratios. Present-day $^{87}Sr/^{86}Sr$ isotope ratios in the glasses range from a minimum of 0·70736 in the Ololbutot centre to a maximum of 0·70795 in the Gorge Farm centre.

The Rb/Sr isotope characteristics of sanidine allow a similar distinction between the eruptive centres (Table 2). Sanidines from lavas erupted at Gorge Farm have $^{87}Rb/^{86}Sr$ ratios between 699 and 771, with near-constant Rb (313–338 ppm) and Sr (1·17–1·40 ppm) concentrations. The difference in Sr isotope composition

Table 2: Rb–Sr, Pb and Nd isotope data for Olkaria (Naivasha) rhyolites

Sample	Rb	Sr	$^{87}Rb/^{86}Sr$	$^{87}Sr/^{86}Sr$	$^{208}Pb/^{204}Pb$	$^{207}Pb/^{204}Pb$	$^{206}Pb/^{204}Pb$	$^{143}Nd/^{144}Nd$
Gorge Farm centre (Group 3; age ≤8 ka)								
504								
gla	731·8	1·311	1615	0·707891±18	39·797	15·815	19·843	0·512565±10
san	313·9	1·177	771·7	0·707425±14	40·045	15·919	19·961	
san*					39·989	15·900	19·867	
565								
gla	662·5	1·307	1467	0·707836±15	39·922	15·848	19·873	0·512568±9
san					39·819	15·866	19·809	
570								
gla	666·6	1·317	1464	0·707860±15	39·821	15·825	19·858	0·512570±7
san	326·1	1·311	720	0·707610±13	39·724	15·835	19·859	
amph	105·8	1·938	158·0	0·707409±13				
bio	1613	3·016	1548	0·709244±15				
GF1								
gla	752·0	1·304	1669	0·707917±12				
san	338·6	1·400	699·7	0·707544±21	39·879	15·873	20·143	
san*					39·637	15·850	19·908	
GF2								
gla	814·0	1·331	1769	0·707950±13	39·803	15·816	19·845	0·512574±13
san	324·9	1·270	740·1	0·707735±18	39·929	15·886	20·194	
san*					39·950	15·886	19·848	
Ololbutot centre (Group 6; age ≤1 ka)								
346								
gla	526·7	2·038	747·7	0·707355±12	39·707	15·817	19·740	0·512521±9
san	144·6	3·413	122·6	0·707257±14				
376								
gla	600·0	2·036	852·6	0·707431±18	39·626	15·794	19·719	0·512508±10
san	146·7	3·262	130·1	0·707283±14	39·581	15·817	19·681	
399b								
gla	517·8	1·979	757·0	0·707365±13	39·677	15·809	19·732	0·512523±9
san	143·5	3·380	122·9	0·707258±13				

gla, glass; san, sanidine; amph, amphibole; bio, biotite.
*Single crystal.

between sanidines and glass ($\Delta^{87}Sr/^{86}Sr$) ranges from $2·2 \times 10^{-4}$ to $4·7 \times 10^{-4}$. Sanidines from the Ololbutot centre have distinctly lower Rb (143–146 ppm) and higher Sr contents (3·26–3·41 ppm) than the Gorge Farm samples. Thus, their $^{87}Rb/^{86}Sr$ ratios are lower (122–130) than those of Gorge Farm sanidines. Differences between sanidines and the coexisting glasses are also smaller ($\Delta^{87}Sr/^{86}Sr = 1·0 \times 10^{-4}$ to $1·5 \times 10^{-4}$). Apparent sanidine–glass partition coefficients for strontium are 0·90–1·07 for the Gorge Farm and 1·60–1·70 for the Ololbutot centre, which indicates that strontium partitioning into sanidines is lower in the compositionally more evolved lavas.

^{230}Th–^{238}U isotope data

Th–U concentrations and calculated activity ratio data for glasses and minerals are given in Table 3. Thorium concentrations of glasses are in the range 90·5–92·8 ppm at the Ololbutot centre and 120·4–157·9 ppm at Gorge Farm. Uranium concentrations are in the ranges 22·8–23·35 and 30·7–39·7 ppm, respectively, resulting in rather uniform Th/U weight ratios in both eruptive centres (3·92–3·98). Thorium isotope compositions are similar ($^{230}Th/^{232}Th = 0·76$–$0·78$), with glasses from Gorge Farm close to secular equilibrium (^{230}Th excess between 0·1 and 0·6%). Glasses from the Ololbutot centre (Fig. 8, below) reveal slightly larger ^{230}Th excesses (up to 3%).

Table 3: Concentration and activity data of U-series disequilibria for Olkaria (Naivasha) rhyolites

Sample	U (ppm)	Th (ppm)	($^{238}U/^{232}Th$)	($^{230}Th/^{232}Th$)	($^{230}Th/^{238}U$)	($^{234}U/^{238}U$)
Gorge Farm centre (Group 3)						
504						
glass	34·12	135·5	0·763 ± 7	0·760 ± 4	1·005 ± 11	0·997 ± 8
sanidine	0·631	2·670	0·715 ± 2	0·748 ± 4	1·044 ± 6	0·992 ± 7
quartz	2·19	9·02	0·737 ± 3	0·751 ± 8	1·037 ± 12	0·997 ± 6
amphibole	3·10	13·61	0·690 ± 3	0·740 ± 3	1·080 ± 6	0·979 ± 5
biotite	1·62	7·90	0·621 ± 3	0·734 ± 11	1·293 ± 19	1·009 ± 12
fayalite	64·83	49·95	3·935 ± 14	1·875 ± 8	0·479 ± 3	0·995 ± 5
magnetite	0·762	3·08	0·751 ± 2	0·755 ± 3	1·013 ± 11	0·994 ± 7
mag. fract.	12·56	50·95	0·748 ± 3	0·750 ± 3	1·012 ± 11	0·990 ± 7
565						
glass	30·73	120·4	0·773 ± 6	0·773 ± 3	1·000 ± 9	0·994 ± 4
570						
glass	32·74	129·5	0·767 ± 4	0·765 ± 4	0·996 ± 7	0·990 ± 8
sanidine	0·577	2·41	0·727 ± 1	0·753 ± 4	1·044 ± 6	0·992 ± 7
amphibole	3·65	14·67	0·754 ± 2	0·764 ± 3	1·019 ± 5	0·982 ± 4
fayalite	4·31	16·25	0·804 ± 2	0·796 ± 9	1·004 ± 11	0·997 ± 6
mag. fract.	7·23	29·76	0·736 ± 1	0·755 ± 3	1·039 ± 4	0·994 ± 7
GF2						
glass	39·77	157·9	0·764 ± 4	0·768 ± 3	1·005 ± 7	0·995 ± 6
Ololbutot centre (Group 6)						
346						
glass	23·35	92·83	0·762 ± 3	0·782 ± 5	1·026 ± 8	0·994 ± 3
376						
glass	23·07	91·52	0·764 ± 6	0·778 ± 4	1·018 ± 10	0·998 ± 6
quartz	1·96	7·82	0·759 ± 2	0·776 ± 4	1·022 ± 6	0·999 ± 8
399						
glass	22·84	90·49	0·765 ± 4	0·778 ± 4	1·017 ± 7	0·996 ± 8

The analysed mineral phases show greater variation in ^{230}Th–^{238}U disequilibrium than the glasses (Fig. 9, below). All minerals, except for one fayalite, have ^{230}Th excesses that range from 1·2% (magnetic fraction of sample 504) to 29% (biotite in 504). The exceptions are the fayalite fractions of sample 504, which record a ^{238}U excess of 52% over ^{230}Th, and fayalite of sample 570, which plots just off the equiline.

($^{234}U/^{238}U$) activity ratios are within error of unity in all but two of the analysed samples and consequently provide no evidence that there has been interaction of the rocks with meteoric or ground waters. Nevertheless, amphiboles from samples 504 and 570 have small (~2%) excesses of ^{238}U.

Pb and Nd isotope compositions

The Pb and Nd data presented in Table 2 establish that glasses from an individual group are indistinguishable but, as shown in Fig. 5, there is a small difference between the Gorge Farm and Ololbutot centres in $^{143}Nd/^{144}Nd$ (0·51257 and 0·51252) and $^{206}Pb/^{204}Pb$ (19·87 and 19·73). The feldspars have variable Pb isotope ratios ($^{206}Pb/^{204}Pb$ = 19·52–20·15). Pb isotopes of feldspars and glasses from the Olobutot centre are identical. In contrast, some bulk sanidine separates from the Gorge Farm centre (GF samples) and a single grain analysis have Pb isotope compositions that are not in Pb isotope equilibrium with the coexisting glasses (Fig. 6). The vectors *b* and *f* in Fig. 6 represent the possible contribution of blank and the

Table 4: Oxygen isotope compositions of glasses

Sample	$\delta^{18}O$ (‰)
Gorge Farm centre (Group 3)	
504	6·66
	6·51
	6·44
565	6·44
	6·46
570	6·80
GF2	6·96
Ololbutot centre (Group 6)	
346	6·80
376	6·28
	6·30
399	6·48

trajectory caused by analytical mass fractionation. These vectors clearly indicate that the isotopic differences are not an analytical artefact. In addition, bulk sanidine separates from the GF samples were the largest, thus they should be the least sensitive to blank contributions.

Oxygen isotope compositions

Laser probe oxygen isotope data are given in Table 4. The $\delta^{18}O$ values of the comenditic glasses vary from 6·2 to 6·9‰ with an average close to 6·6‰, indicating no obvious difference in isotopic composition between the eruption centres.

DISCUSSION

Individuality of eruptive centres

The rhyolites of the Greater Olkaria Volcanic Complex record large variations in trace element and isotopic characteristics. This observation is perhaps surprising for volcanic rocks of very similar major element composition, erupted in close vicinity and over a relatively short time scale (<20 ky). Although many bulk compositional features are shared with rocks of other centres, there are features, especially trace element and isotopic ratios, that characterize products from individual eruptive centres, for example, the Gorge Farm and Ololbutot centres (Fig. 3). Macdonald *et al.* (1987) modelled the compositional variations within individual comendite groups as predominantly a consequence of fractional crystallization.

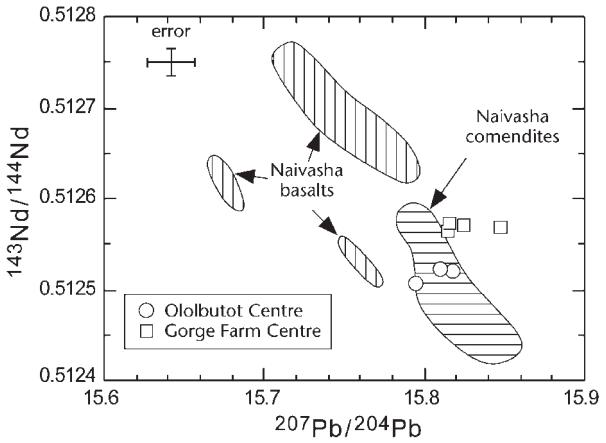

Fig. 5. Pb and Nd isotope compositions of analysed comenditic glasses. Fields with hatch-pattern are for volcanic rocks at the Olkaria Volcanic Complex (Davies & Macdonald, 1987).

We concur that extremely low Sr concentrations and coherent Zr–Nb variations are best modelled by fractional crystallization of the observed phenocryst populations (e.g. alkali feldspar fractionation; Halliday *et al.*, 1991). Differences between the groups, however, require the contribution of other processes or the involvement of different magmatic lineages. Hence the model was previously proposed calling upon partial melting or source effects to account for the subtle variations between centres and chemical groups. In strong support for such a model are variations in the Sr–Nd–Pb data, which correlate with trace element ratios (e.g. $^{143}Nd/^{144}Nd$ and Zr/Nb ratios; Davies & Macdonald, 1987). Three isotopic components were identified involving Pan African basement and the volcaniclastic infill of the rift valley. The inferred crustal lithologies beneath Olkaria range from felsic to mafic gneisses, formed under amphibolite- to granulite-facies conditions (Mooney & Christensen, 1994). Despite the variation in potential crustal source rocks, it must be noted, however, that the strong depletion in typical crustal elements (e.g. Ba and Sr) in the comendites demands significant chemical fractionation after initial melting (see also next section).

The Sr–Nd–Pb isotope results obtained from glasses in this study (Table 2; Figs 5 and 6) are indistinguishable from the results of Davies & Macdonald (1987) and confirm the individuality of the Gorge Farm (Group 3) and Ololbutot centres (Group 6) in terms of their Pb and Nd isotope ratios. Oxygen isotope compositions of the two studied chemostratigraphic groups are, however, closely similar (Table 4). The $\delta^{18}O$ values are relatively low considering the vast range of potentially high-$\delta^{18}O$ crustal source rocks for the comendites. The $\delta^{18}O$ values probably indicate a relatively low-^{18}O signature of the initial source and/or magma interaction with low-$\delta^{18}O$ lower crust early during the evolution of the comenditic

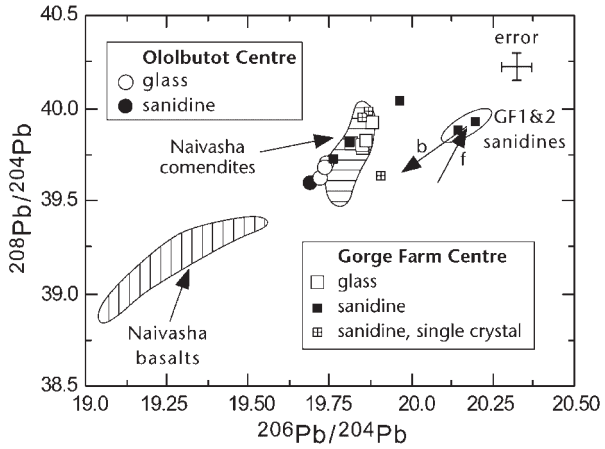

Fig. 6. $^{208}Pb/^{204}Pb$ vs $^{206}Pb/^{204}Pb$ variations for glasses and sanidines of the Gorge Farm and Ololbutot eruption centres. Reference fields from Davies & Macdonald (1987). Arrows indicated with b are mixing trend with analytical blank ($^{206}Pb/^{204}Pb = 17{\cdot}75$, $^{208}Pb/^{204}Pb = 37{\cdot}65$) and those indicated with f are mass fractionation trajectory.

melts, and that fractional crystallization hereafter probably increased the $\delta^{18}O$ values only by $\sim 1‰$. This conclusion implies that the magmas probably inherited their slightly different Sr–Nd–Pb isotope characteristics, even for contemporaneous chemical groups, at an early stage of petrogenesis. Thus, each eruptive centre was fed from individual magma batches, which apparently record slightly different magmatic histories. The configuration of the magma supply system consequently demands spatial separation of small magma chambers in which genetically related melts evolved. To preserve the significant compositional characteristics of each magma suite, there cannot have been significant mixing between the chambers, at least during the final phases of melt evolution. Therefore the existence of a larger, rhyolitic magma chamber beneath the Olkaria Volcanic Field, as proposed by Clarke *et al.* (1990), is not supported by the chemical and isotopic data.

Rb–Sr fractionation and age information

The Rb/Sr ratios of the comendites of Groups 3 and 6 range between 258 and 611 (Table 2). Given that it is possible to resolve differences of $\sim 10^{-5}$ in measured $^{87}Sr/^{86}Sr$ ratios, a maximum age resolution of between 1 and 2 ka could be theoretically achieved for the Rb–Sr isotope system in these samples.

In a Rb–Sr isochron diagram, glasses from both chemical groups define linear relationships equivalent to ages older than the actual eruption event (Fig. 7). The old lavas of the Gorge Farm centre (~ 8 ka) fall on a Rb–Sr isochron indicating an apparent age of 22 ± 4 ka, whereas the recent (<1 ka) lavas from the Ololbutot fissure eruption yield an isochron of 50 ± 15 ka. For the Gorge Farm centre the glass-isochron age appears to be confirmed by a mineral isochron (24 ± 1 ka) of sample 570 (glass, sanidines and amphiboles). If truly isochrons, these data place stringent constraints on magmatic processes. The event documented by the isochrons must have occurred rapidly (± 1 ky), i.e. within the time defined by the error in the isochrons. Subsequent to isochron formation, mineral crystallization or mixing must have been limited, to preserve the isochron relationships. Sanidines from the remaining samples, however, do not plot on the isochrons and define apparent glass–sanidine ages (Table 5) between 15 ± 2 ka and 39 ± 4 ka (Gorge Farm) and around 12 ± 5 ka (Ololbutot centre). In summary, these results indicate Sr isotope differences that can be interpreted as age differences between eruption and the Rb–Sr isochrons of 7–31 ky. Nevertheless, the conspicuous Pb isotope disequilibrium between glasses and sanidines for GF samples casts doubts on the validity of the Rb–Sr age information and on the suggestion that the Rb–Sr fractionation in these lavas is predominantly related to fractionation of these particular sanidine populations. Hence, the processes responsible for the spread in Rb/Sr ratios of glasses have to be evaluated more thoroughly.

Possible causes of Rb–Sr fractionation

A feature of the geochemistry of the comendite glasses from the various groups at Olkaria is their extremely low and constant Sr contents of 1·3 or 2 ppm, as opposed to variable Rb concentrations (Table 2). This consistency raises the question as to which processes other than fractional crystallization could have produced the Rb/Sr ratios. The idea of melt–vapour partitioning for peralkaline systems, involving vapour-phase transport of certain elements or volatile complexing, has been advocated by some workers (e.g. Bailey & Macdonald, 1975, 1987; Baker & Henage, 1977; Macdonald, 1987; Macdonald *et al.*, 1987).

One mechanism proposed to explain pre-eruptive Rb–Sr ages is the preferential contamination by a crustal melt that has radiogenic Sr and is Rb rich (Knesel *et al.*, 1999). This mechanism was proposed because highly evolved rocks, such as the Olkaria comendites, are extremely sensitive to the addition of any crustal lithology. Changing the $^{87}Rb/^{86}Sr$ ratio from 1464 (sample 570) to 1769 (sample GF 2) by any bulk assimilation or addition of partial melt will also increase the Sr content of the rhyolitic melt. In addition, the constant Nd–Pb isotope ratios of the glasses argue against contamination by wall-rocks, although the high Nd and Pb concentrations in the comendites do not make them particularly sensitive to the effect of small amounts of crustal assimilation. Notably biotite, a potential high-Rb mineral in country

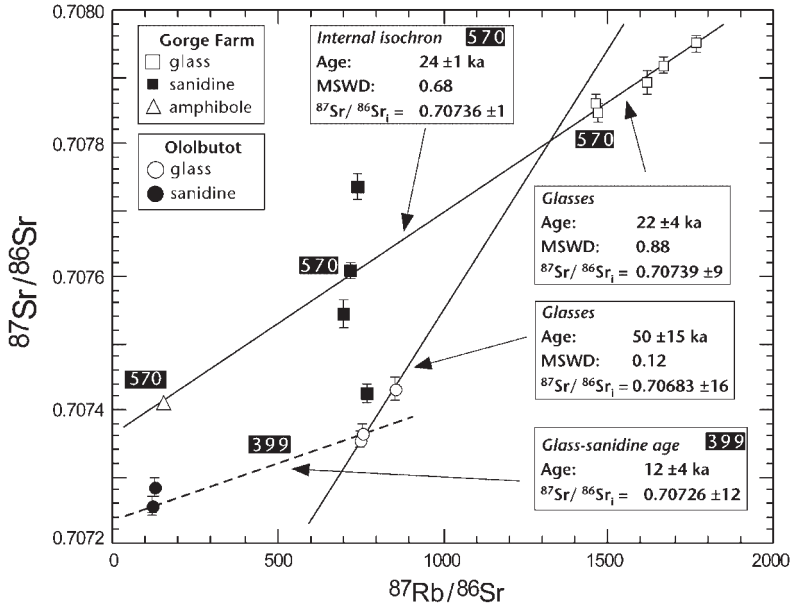

Fig. 7. Rb–Sr isochron diagram of glasses and minerals from the Gorge Farm and Ololbutot eruptive centres. Isochrons and related age information are for glasses only. Mineral–glass ages are listed in Table 5. It should be noted that biotite of 570 plots off scale and not on the isochron. (See text for discussion.)

Table 5: Summary of Rb–Sr age relationships (ka) between glasses and minerals

Sample	Isochron	$^{87}Rb/^{86}Sr$ age	MSWD	$^{87}Sr/^{86}Sr_i$
Gorge Farm centre (Group 3)				
504, 565, 570, GF1, GF2	glasses	22±4	0·88	0·70739±9
570	glass, san, amph	24±1	0·68	0·70736±1
570	glass, san	24±2	—	0·70737±3
504	glass, san	39±4	—	0·70700±3
GF1	glass, san	27±4	—	0·70727±4
GF2	glass, san	15±2	—	0·70758±3
Ololbutot centre (Group 6)				
346, 376, 399	glasses	50±15	0·12	0·70683±16
346	glass, san	11±4	—	0·70724±2
376	glass, san	14±4	—	0·70726±2
399	glass, san	12±4	—	0·70724±12

san, sanidines; amph, amphiboles.

rocks, is a stable phase in the more peralkaline comendites, precluding selective incorporation and assimilation of this phase to explain Rb–Sr variations observed in the glasses (e.g. Knesel *et al.*, 1999). Therefore we conclude that there is no chemical or petrographic evidence that supports crustal contamination or combined assimilation and fractional crystallization.

Peralkaline silicic rocks are prone to compositional changes during crystallization or secondary hydration of glasses. Degassing processes on crystallization, notably involving halogens (F, Cl), have been argued to be responsible for increased element mobilities of Na, Sr, Cs, Y or REE (Baker & Henage, 1977; Weaver *et al.*, 1990). Secondary hydration of peralkaline rhyolites from the Olkaria complex would be accompanied by compositional changes involving Sr or Pb gains and modification of their isotope systematics (Davies & Macdonald, 1987). Both potential effects can be excluded for the nearly aphyric rocks of the present study as they consist entirely of non-hydrated glass. Hydration would dramatically alter the very low Sr concentrations and possibly cause isotopic disequilibrium between the ^{234}U–^{238}U radionuclide pair (see following sections). Consequently, post-eruptive element mobility is highly unlikely in the present samples and hence their element and isotope characteristics can be regarded as magmatic.

Nevertheless, it has been established that some of the rhyolites of the Greater Olkaria Volcanic Complex experienced pre-eruptive degassing with an unknown amount of volatiles loss (Wilding *et al.*, 1993). There are no apparent correlations between volatile and element concentrations or isotopic signatures (Macdonald *et al.*, 1987; Black *et al.*, 1997). Degassing processes theoretically could have severe consequences for those elements that

are suspected to form mobile halogen-complexes (e.g. Flynn & Burnham, 1978; Davies & Macdonald, 1987). If Rb, for instance, was assumed to be selectively fractionated by a process that at the same time did not affect Sr, then melts, degassed to different degrees, could attain varying Rb/Sr ratios. Upon radioactive decay, the Rb–Sr isotope system would record the time that elapsed since this event. In such a scenario, any age information would point to the last chemical fractionation of these melts in the same way as Rb–Sr fractionation caused by crystal–melt processes, i.e. feldspar fractionation. However, trace elements record coherent correlations that imply no preferential loss of trace elements through volatile loss (Table 1; Fig. 4). Formation of volatile complexes in the melt may make some trace elements more incompatible in silicate phenocrysts leading to more incompatible behaviour during fractional crystallization, i.e. the process will mimic fractional crystallization but suggesting greater degrees of mineral separation. The effect of exsolving magmatic vapour from peralkaline melts therefore remains difficult to assess in detail. From the available data, volatile complexing during the final melt evolution does not appear to have been a significant process in producing the trace element characteristics of the comendites. Volatiles, however, possibly play an important role during the initial melting in the source regions (Macdonald *et al.*, 1987).

Rb–Sr fractionation by minerals

The internal glass–sanidine–amphibole isochron for sample 570 records mineral crystallization ages of 24 ± 1 ka (Fig. 7; Table 5) and apparently supports the age information of 22 ± 4 ka recorded by all Gorge Farm glasses. Inferred partition coefficients are in the range of reported values (Drexler *et al.*, 1983; Mahood & Stimac, 1990) and suggest that the spread of $^{87}Rb/^{86}Sr$ ratios documented in the glasses was controlled by crystal fractionation of the observed mineral phases. This conclusion, however, is not supported by all samples. For example, biotites from sample 570 do not fall on the internal isochron. This could be the consequence of two possible processes: (1) the presence of xenocrystic biotite, despite the phenocrystic appearance and lack of compositional variation in the biotite (Macdonald *et al.*, 1987) or (2) diffusive exchange between biotite and melt, displacing biotite from the glass–sanidine–amphibole trend. It is perhaps significant that biotite also does not fall on the pre-eruptive isochrons, as in the Long Valley system (Davies *et al.*, 1994), suggesting that biotite does not remain a closed system for Rb and/or Sr during long periods of residence in a magma.

Sanidines from other samples of the Gorge Farm centre have Rb–Sr isotope characteristics that may indicate sanidine crystallization over a 24 ky period (Table 5). However, sanidine populations from samples 504, GF1 and GF2 reveal $^{206}Pb/^{204}Pb$ ratios higher than the respective glasses and clearly outside the range described by all the comendite groups (Davies & Macdonald, 1987). Euhedral sanidine crystals from the Olobutot centre have Pb isotope ratios identical to the host glasses, but the sanidine–glass Rb–Sr ages yield younger results than the glass isochron and are still significantly older than the eruption ages. This implies that either they crystallized at ~12 ka or have a xenocrystic origin. The results for the observed sanidine assemblages therefore must be interpreted with caution. Pb isotope ratios suggest that part of the sanidine population could be xenocrystic in origin. Given the radiogenic nature of some feldspars, it appears probable that they have been derived from the Miocene to Recent volcanic rocks that form the majority of the upper 6 km of the rift valley (Norry *et al.*, 1980; Macdonald *et al.*, 1987). Nevertheless, the isotopic heterogeneity of sanidines contrasts with their euhedral crystal shapes and composition, which appears to be typical for feldspars crystallized from peralkaline magmas (Macdonald *et al.*, 1987). Additionally, Rb–Sr element partitioning into the sanidines is coherent and sanidines from the two groups have distinctive compositions (Group 3: Rb 313–338 ppm, Sr 1·17–1·40 ppm; Group 6: Rb 143–147 ppm, Sr 3·26–3·41 ppm), implying a single common parent for each group.

Partition coefficients for Sr and Rb in alkali feldspars are related to melt peralkalinity and orthoclase component (i.e. Drexler *et al.*, 1983; Mahood & Stimac, 1990). Thus, the relatively low Sr content of the sanidines is in agreement with the chemical compositions of the glasses. The low partition coefficients, close to unity, cannot be solely responsible for the strong Sr depletion in the comendites. It is possible, however, to relate the degree of Rb–Sr fractionation in the glasses to fractionation of the observed feldspar populations. To produce the most fractionated melt (sample GF2) from the least evolved in Group 3 (sample 570), ~33% fractionation of sanidines is required ($D^{Rb} = 0{\cdot}4$; $D^{Sr} = 1$). This amount of sanidine fractionation is lower than the 56% sanidine fractionation deduced from major element modelling, assuming formation of Group 3 rocks from the least evolved rhyolites of Group 1 (Macdonald *et al.*, 1987). The fractionating assemblage in Group 3 comendites is dominated by sanidines with a Sr partition coefficient close to unity, which explains the apparently constant Sr concentration in the glasses. Even relatively large amounts of fractionation will cause little increase in Sr contents, as observed in sample GF2, which has the highest Sr concentrations in Group 3. The different Pb isotope compositions of some sanidines in samples GF 1 and 2, however, raise the possibility that not all 'phenocrysts' grew from melts represented by the host glasses. These

sanidines probably originated from peralkaline magmas, because their Rb–Sr compositions are identical to other sanidines from Group 3 rocks. The processes that incorporated the sanidines into the GF1 and 2 melts remain poorly constrained. The above observations favour an origin of the sanidines from compositionally similar, though isotopically distinct, magmas. This conclusion is consistent with feldspar incorporation from within the volcanic pile during eruption. Constant Pb–Nd isotope compositions of lavas from individual eruptive centres at Naivasha preclude significant mixing to produce the Rb–Sr variations. Thus the most plausible interpretation of the Rb–Sr systematics of the lavas is that most of the mineral crystallization of a sanidine-dominated mineral assemblage occurred at 24 $\pm$ 1 ka (internal isochron sample 570; Fig. 7). Subsequently, there was minor incorporation of material from the volcanic pile, probably during eruption. This process, however, did not significantly affect the Rb–Sr systematics of the whole rocks or glasses.

^{230}Th–^{238}U disequilibrium

The Sr–Nd–Pb isotope results discussed above highlight a complex petrogenesis for the Olkaria rhyolites. Although the isotopic individuality of the eruptive centres possibly points to the influence of diverse lithospheric sources, their element variations and low Sr contents require significant fractionation within each eruptive centre. Consequently, the U–Th fractionation and the U-series disequilibrium documented in the Olkaria rhyolites could be the result of a combination of processes during their genesis. It must therefore be established if the intragroup variations are a consequence of U/Th fractionation being controlled by (1) source effects with a dominantly crustal contribution (initial melting and/or assimilation of lower crust) or (2) chemical fractionation during final magma evolution.

Previous work

In a recent study by Black *et al.* (1997), the U–Th disequilibrium of a large number of Olkaria rhyolites was measured by alpha spectrometry. Those workers proposed a model in which the degree of U–Th fractionation of the comendites is predominantly a consequence of volatile-induced melting of crustal source rocks. They further argued that the peralkalinity of the melts controls zircon stability in the residual source mineralogy. Despite their conclusion, Black *et al.* (1997) also reported internal U–Th isochrons for the Middle and Upper Comendite Members (including samples from the Gorge Farm centre), which were interpreted as pre-eruptive phenocryst crystallization ages. No clear quantitative distinction, however, was made between the extent to which the fundamentally different fractionation mechanisms relate to each other and how they contributed to the observed U–Th disequilibrium. In particular, Black *et al.* argued that fractional crystallization of the observed mineral phases can produce only minor U–Th fractionation. They drew this conclusion from the inability of their U–Th mineral data to explain whole-rock U–Th variations. Furthermore, a proposed negative correlation between inferred crystallization ages and the zirconium content of whole rocks led them to reject fractional crystallization as the dominant process for generating the rhyolites. This conclusion, however, is inconsistent with respect to their interpretation of the U–Th mineral isochrons having age significance. In peralkaline melts, zircon is not a stable mineral phase and zirconium behaves as an incompatible element (Watson, 1979). Consequently, the inverse relationship between Zr content and U–Th age is fully consistent with progressive melt evolution of peralkaline rhyolites, i.e. the most evolved rocks formed later. This conclusion is also in agreement with the low Sr and Ba contents of the comendites, which require extensive mineral fractionation and exclude crustal assimilation of zircon-bearing wall-rocks to explain the zirconium and U–Th variations.

Having apparently ruled out the potential effects of fractional crystallization in their interpretation of the U–Th disequilibrium data, Black *et al.* (1997) closely followed the volatile-fluxed partial melting model of Macdonald *et al.* (1987). The majority of their whole-rock data show ^{238}U excesses, plotting to the right of the equiline. Thus by drawing parallels to fluid-controlled fractionation of U from Th during subduction-related magmatism (Gill & Williams, 1990), Black *et al.* stressed the importance of source metasomatism by halogen-rich fluids for the U enrichment and genesis of the comendites. Additionally, they proposed that the occurrence of zircon in the oldest, least evolved comendites and its absence with increasing peralkalinity in younger rhyolites, in combination with a positive correlation between U–Th disequilibrium and pre-eruptive F content, indicate melting out of zircon in the source rocks. Hence they argued that U–Th fractionation during an initial crustal melting process explains the disequilibrium data.

Below it will be argued that the range of the U–Th disequilibrium data of whole rocks is equally compatible with, and more easily explained by, a petrogenesis dominated by fractional crystallization.

Origin of U–Th fractionation

Whereas Black *et al.* (1997) studied an impressively large number of samples from nearly all eruptive centres at

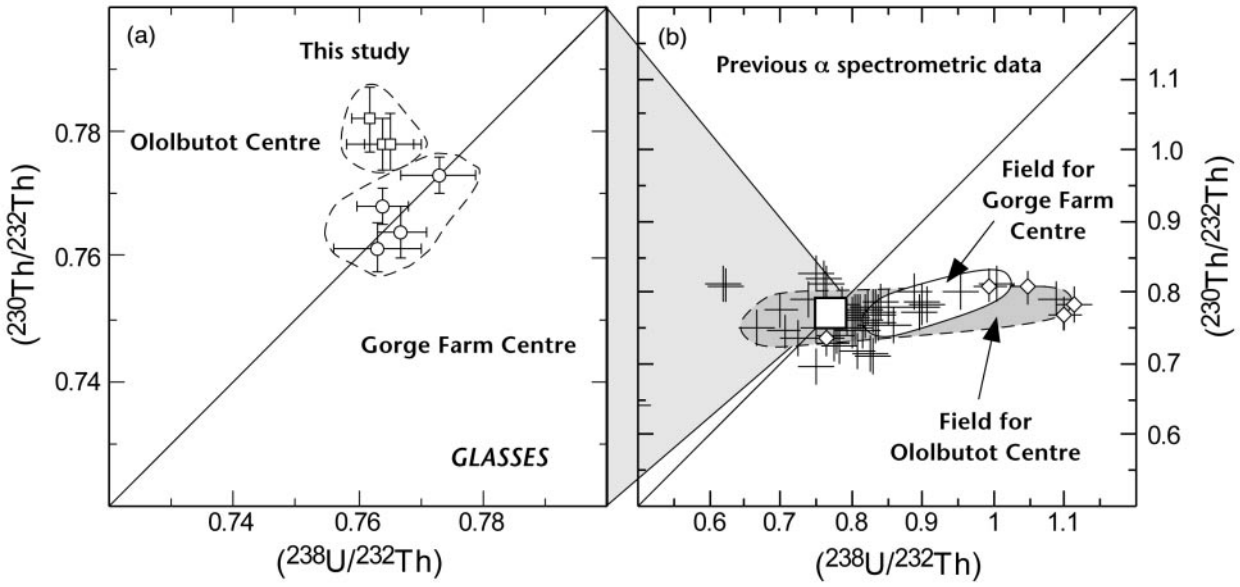

Fig. 8. U–Th equiline diagram of glass analyses from this study (a) compared with the previously published alpha spectrometric data (b) for all the comendite whole-rock analyses of Black *et al.* (1997). The data of (a) are depicted as a white square in (b). Reference fields in (b) are drawn for whole-rock analyses of the Gorge Farm and the Ololbutot centre. ◇, glass analyses for Gorge Farm by alpha spectrometry (Black *et al.*, 1997). It should be noted that the range of U/Th ratios in these glasses is larger than in host whole rocks. The symbol size of the alpha spectrometric data corresponds to the reported mean 2σ error of Black *et al.* (1997). (See text for further discussion.)

Olkaria, only the most differentiated comendites from two groups are the subject of the present investigation. This restricts the interpretation of the data to the variations within restricted parts of those separate eruptive centres and limits conclusions with respect to the genesis of the entire comendite field. Importantly, however, the U–Th disequilibrium data of glasses and minerals obtained in this study on identical samples are only partly in agreement with the results from the alpha spectrometry study of Black *et al.* (1997). Although the Th isotopic compositions measured by TIMS fall within the accuracy of the alpha spectrometric data, the range of U/Th ratios and hence the degree of U-series disequilibrium reported by Black *et al.* (1997) cannot be confirmed.

TIMS vs alpha spectrometry

Figure 8 represents an overview of the U–Th disequilibrium for glass analyses by TIMS obtained in this study compared with the published alpha spectrometric data for the Olkaria Volcanic Complex (Black *et al.*, 1997). The TIMS measurements (Table 3; Fig. 8a) show that disequilibria of glasses are indistinguishable within each eruption centre (Gorge Farm; Ololbutot), but that there is a slight difference between the centres. Glasses from the Gorge Farm centre plot on the equiline, whereas glasses from the Ololbutot centre have slightly higher Th isotopic compositions and ^{230}Th excesses, plotting to the left of the equiline. Thus minor U–Th disequilibrium of the comenditic melts is indicated only for the Olobutot centre.

The isotopic homogeneity of glasses measured by TIMS is in marked contrast to the range of U/Th variations obtained by alpha spectrometry (Fig. 8b). The difference cannot be explained by the greater precision of the TIMS data because the alpha spectrometry data are significantly outside analytical error. All alpha spectrometric whole-rock and glass analyses from Gorge Farm reveal ^{238}U excess (Black *et al.*, 1997). Only one of their five glass analyses for the Gorge Farm centre (566) has (^{238}U/^{232}Th) and (^{230}Th/^{232}Th) activity ratios within error of the TIMS measurements. The remaining glasses have U/Th ratios notably higher than even the respective whole-rock analyses. Larger sample sizes are required for alpha spectrometry, which may have resulted in impure glass separates. Therefore, the much smaller amount of separated glass used for TIMS analysis may account for the much more homogeneous isotopic results, but does not fully explain the large spread in the alpha spectrometric U–Th data. Further speculation on the analytical differences is impossible without detailed knowledge of the dissolution procedures used and yields obtained in the alpha spectrometry technique.

The new and fundamentally different TIMS results, however, have important consequences for the petrogenetic interpretation of the U–Th disequilibrium of the

Olkaria comendites. The U–Th isotopic compositions of glasses from the Gorge Farm centre are all in secular equilibrium. This suggests that either U and Th were not significantly fractionated during a melting-related petrogenesis or that the melts are older than 350 ka. Hence, U–Th isotopic compositions of the Gorge Farm glasses alone provide little information on their genesis. In contrast, the stratigraphically younger comendites of the Ololbutot fissure eruption document small Th excesses. Thus, melt compositions (glasses) possibly plot on both sides on an equiline diagram [taking into consideration that not all eruptive centres are investigated in this work (Fig. 8)]. This requires that U–Th fractionation was caused by processes in the source that affected both U and Th concentrations or that minerals with notably different partition coefficients for U and Th were involved in the petrogenesis. These observations strongly indicate that the volatile-induced U-enrichment process postulated by Black *et al.* (1997) cannot be the sole mechanism operating during the petrogenesis of the Olkaria comendites.

U–Th fractionation upon melting

The comprehensive publications on the Olkaria comendites have provided ample evidence of crustal involvement during comendite genesis (Davies & Macdonald, 1987; Macdonald *et al.*, 1987; Black *et al.*, 1997). There are also unequivocal indicators, however, that the parental magmas experienced significant modification leading to low Sr and Ba concentrations. These features clearly preclude significant crustal contamination, i.e. equilibrium wallrock melting in the magmatic feeding system adding significant amounts of Sr is not a major process in producing the compositional variations of the comendites. U–Th disequilibrium is therefore assessed in terms of the initial melting process and/or subsequent element fractionation during magmatic evolution.

^{238}U–^{230}Th radioactive disequilibrium upon melting depends chiefly on the melting mode, the presence of accessory minerals with significantly distinct U/Th ratios and the isotopic composition of the crustal source (Gill, 1993). In spite of the potential influences of crustal melting for U–Th fractionation, the glasses of the two studied eruptive centres have ($^{238}U/^{230}Th$) ratios surprisingly close, or equal, to secular equilibrium. At the Gorge Farm centre, this suggests that the differentiation processes related to melting either produced no fractionation of U from Th and the duration of melting and transport were rapid or that the comendites represent old melts (initially in or out of radioactive equilibrium) that have returned to radioactive equilibrium. In the context of crustal melting, the small ^{230}Th excess over ^{238}U for glasses from the Ololbutot centre could indicate a number of possible melting scenarios. The glasses analysed in this study, however, have constant Th/U ratios (3·92–3·98), despite large variations in U and Th concentrations in Gorge Farm glasses (U 31–40 ppm; Th 120–160 ppm) and the much lower U–Th concentrations in the Ololbutot glasses (Table 3). It requires special pleading to produce a constant U/Th ratio and variable U and Th concentrations by melting of either a single source or separate source regions involving various amounts of minor mineral phases (e.g. zircon, allanite, monazite). In addition, the compositional variety of comendites erupted over a period of 20 ky is difficult to reconcile with prolonged crustal melting of a source that remained close to radioactive equilibrium. The combined Sr–Nd–Pb data clearly preclude a single source. We therefore conclude that modification of crustally derived melts by fractional crystallization appears to be the most plausible explanation for the U-series characteristics of the Olkaria comendites.

U–Th variations by mineral crystallization

The role of fractional crystallization during the magmatic evolution of the Olkaria rhyolites has been assessed previously by modelling combined major- and trace-element (REE, Zr, Nb) variations (Macdonald *et al.*, 1987). Despite acknowledging the isotopic characteristics, which demand additional petrogenetic processes, if not separate magma batches (Davies & Macdonald, 1987), Macdonald *et al.* (1987) showed that the compositional variations from the least to the most evolved comendites could be explained by 83% fractionation of an alkali feldspar and quartz dominated mineral assemblage. In addition, the absolute range of Zr–Nb concentrations concurs with such a degree of fractional crystallization. Variations in Zr/Nb ratios, however, indicate that fractional crystallization must have operated independently in the various comendite groups. In contrast, Macdonald *et al.* (1987) argued against a role for accessory phases and interpreted the REE characteristics of the comendites to be incompatible with the fractional crystallization model.

The exceedingly strong enrichment in elements such as Zr, Nb, Ta, U, Th, REE, F and Cl is related to high saturation levels for these elements, low melt polymerization and modified melt structures in peralkaline melts (Watson, 1979; Keppler, 1993; Peiffert *et al.*, 1996; Webster & Rebbert, 1998). Quartz and feldspar fractionation will consequently lead to residual melts that become increasingly enriched in these constituents. The saturation behaviour of peralkaline melts will exert strong control on the variability of element contents by affecting the stability of accessory mineral phases that could potentially deplete the magma in trace elements. To fully

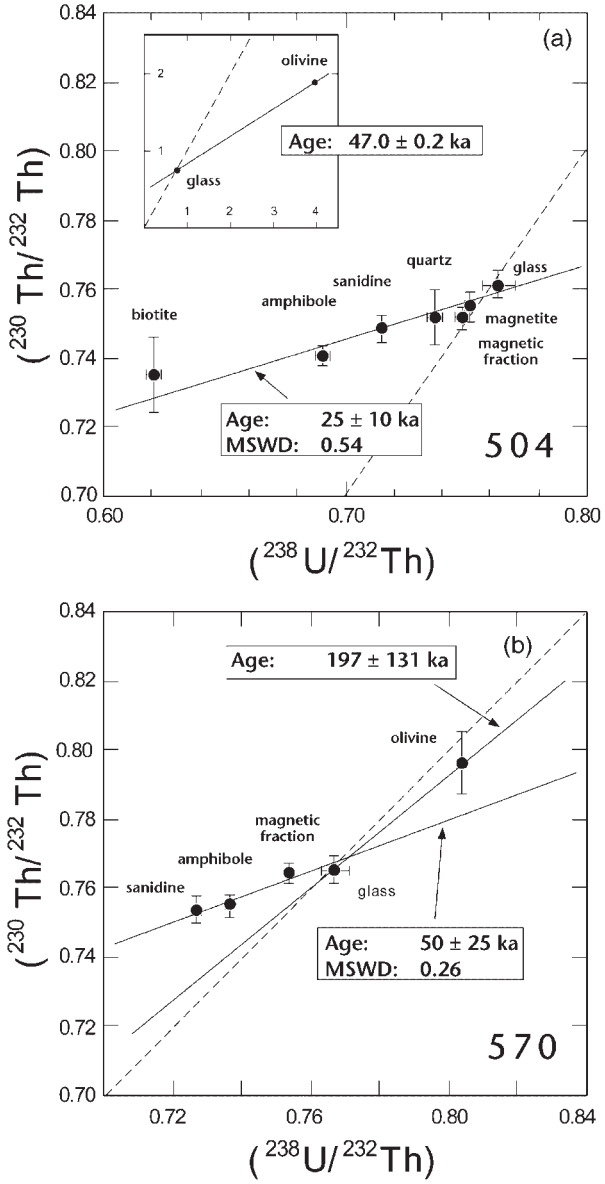

Fig. 9. ^{230}Th–^{238}U mineral isochrons for Gorge Farm comendites 504 (a) and 570 (b) erupted ~8 ky ago. Dashed lines are equilines. (See text for discussion.)

assess the importance of fractional crystallization, the U–Th data of minerals and the role of minor phases have to be included in the discussion of trace element modelling.

The ^{230}Th–^{238}U disequilibrium data for minerals from the Gorge Farm centre are presented in an equiline diagram in Fig. 9. In contrast to the previously discussed glasses, which are in radioactive equilibrium, the analysed mineral phases biotite, amphibole, sanidine, quartz and magnetite show in decreasing order ^{230}Th excesses with respect to ^{238}U and plot to the left of the equiline. Fayalite from sample 504 (Fig. 9a) has a significantly different (^{238}U/^{232}Th) ratio of 3·9 and a higher Th isotope composition [(^{230}Th/^{232}Th) = 1·88]. Similarly, fayalite in sample 570 (Fig. 9b) has a slightly higher U–Th ratio than the glass, although much less extreme than in sample 504, and plots close to the equiline. The topology of the mineral data appears to be similar to the Black *et al.* (1997) data for Gorge Farm samples except for the different (^{238}U/^{232}Th) ratios; that is, the alpha spectrometric mineral data plot mainly to the right of the equiline. This discrepancy will be further examined below.

The high U–Th element concentrations and apparent disequilibrium of mineral phases such as quartz and sanidine suggest that other, undetected minerals might be present in the mineral separates. Macdonald *et al.* (1987) reported the scarce occurrence of clusters of pyroxene and magnetite with zircon and apatite in the oldest, least peralkaline rhyolites (Lower Comendite Member). Chevkinite, another LREE-enriched accessory phase, is apparently present in rhyolites from the Gorge Farm centre, occurring in equal amounts (0·15% by mode) to fluorite (Marshall *et al.*, 1998). Such accessory phases have a great potential for U–Th fractionation because of their high capacity to readily accommodate large amounts of U (zircon) or Th (allanite, chevkinite). Chevkinite is a Ti–REE-rich accessory phase, often reported from peralkaline rocks (e.g. Michael, 1983; Wolff & Storey, 1984), and assumed to play an important role, similar to allanite, in controlling the abundances of LREE and other trace elements (e.g. Th, Ta, Nb, Zr) in evolving magmas (Green & Pearson, 1988). The occurrence of these accessory mineral phases, which are difficult to detect in thin sections, strongly influences the U–Th disequilibrium of analysed glass or mineral separates. The high Th/U ratios of minerals plotting to the left of the equiline (Fig. 9) therefore strongly imply the presence of chevkinite as inclusions in controlling the Th enrichment of these phases.

In conclusion, REE and U–Th data indicate the presence of an accessory mineral phase that preferentially incorporates Th and the LREE. This phase, chevkinite, strongly controls the production of U–Th disequilibrium of the major minerals. Thus, the variability of U–Th disequilibrium in the minerals is fully compatible with mineral crystallization (Fig. 9) of the observed phases.

Isochron ages

In the equiline diagrams in Fig. 9, the internal ^{230}Th–^{238}U isochrons of samples 504 (Fig. 9a) and 570 (Fig. 9b) define mineral–glass arrays equivalent to pre-eruptive ages that pre-date the actual onset of subaerial magmatic

activity at the Olkaria Volcanic Complex (20 ka). In sample 504, there is a clear distinction between a relatively old age defined by fayalite (fayalite–glass relationship indicates an age of 47 ± 0·2 ka) and a younger age (25 ± 10 ka) for the minerals excluding the fayalite (Fig. 9). Similar relationships for sample 570 indicate an age of 197 ± 131 ka and 50 ± 25 ka, respectively. The older ages for each sample are clearly dominated by the disequilibrium data for fayalite that deviate from the general linear trend of the remaining analysed phases. The fayalite of sample 504 (Fig. 9a) has an extreme U–Th ratio, which results in a good age resolution (±0·1 ka). The fayalite separate in sample 570 (Fig. 9b) has a less extreme U–Th ratio but also plots above the linear trend defined by the remaining phases. These characteristics of fayalite strongly contrast with the disequilibrium of the glasses and the ^{230}Th excesses, relative to ^{238}U, recorded by the other minerals.

Initially, the fayalite is omitted from the discussion. Relatively high U and Th element concentrations in the relevant minerals may in part be related to the highly enriched nature of the comenditic melts. Such high concentrations, however, are obviously not caused by glass (melt) inclusions, as commonly assumed (e.g. Black *et al.*, 1997), because the (^{238}U/^{232}Th) ratios of these minerals clearly differ from that of the glass. An alternative explanation for the trend of decreasing (^{238}U/^{232}Th) from glass to biotite (Fig. 9a) or sanidine (Fig. 9b) could be a greater contribution of mineral inclusions with high partitioning for thorium. As mentioned in the preceding section, chevkinite is present in lavas erupted at the Gorge Farm centre (Marshall *et al.*, 1998). The high Th concentrations of chevkinite (e.g. ThO_2 1·5 wt %; Verplanck *et al.*, 1999) and its presence in the mineral separates can easily account for the formation of the isochrons, the high element concentrations and the decreasing (^{238}U/^{232}Th) of minerals. This assumption appears to be confirmed by the results of an initial ion-probe study, which indicates Th/U ratios of 50:1 for the chevkinites from these rocks (R. Macdonald, personal communication, 1999).

Other mechanisms that could create the linear trend in Fig. 9, such as a residual origin of minerals, mixing of mineral populations from different magmas or a combination of these processes, are very difficult to reconcile with the coherent results from the two separate samples 504 and 570 or other samples analysed by Black *et al.* (1997). The euhedral habit of the minerals and their chemical compositions typical of peralkaline rhyolites (Macdonald *et al.*, 1987) preclude an interpretation as residual fragments from the source. In addition, the fact that the melts (glasses) are in secular equilibrium suggests large degrees of initial melting, which makes it very difficult for residual phases to be preserved. Mixing amongst minerals from different magmas must be limited because of the distinct Sr–Nd–Pb isotope and trace element characteristics of magma groups at the Olkaria Volcanic Complex. It requires special pleading to mix variable mineral proportions from two magmas at the required percentages to obtain a consistent linear relationship. In contrast, inclusion into the major phenocryst phases of variable amounts of Th-rich chevkinite appears to be the most probable explanation for the mineral data plotting to the left of the equiline, and hence the array corresponds to the crystallization age of chevkinite.

Nevertheless, chevkinite cannot be held responsible for the anomalous fayalite data, which define ages older than the previously discussed mineral–glass array (Δ^{230}Th–^{238}U age = 11 ka). Although in the literature there are only limited U-series data for fayalites from evolved rocks (e.g. Bourdon *et al.*, 1994), it seems very unlikely that the extremely high (^{238}U/^{232}Th) and (^{230}Th/^{232}Th) ratios in sample 504 represent the U-series systematics of fayalite. This assumption is also supported by the distinctly different fayalite data from sample 570 (Table 3; Fig. 9). The high activity ratios for fayalite in sample 504, when taking into consideration the high U–Th element concentrations, are similar to values obtained from zircons (Heumann, 1999) and may therefore suggest that zircon (or another U-rich phase) is present in this fayalite separate. On the assumption that fayalite contains vanishingly little U and Th (Bourdon *et al.*, 1994), only 0·1 wt % zircon in the 200 mg fayalite separate can account for a shift of (^{238}U/^{232}Th) from equilibrium (glass composition) to the 3·6 value. The required 200 μg of zircon would correspond to a 100 μm spherical zircon crystal (600 ppm U) or equally to several smaller grains.

The presence of zircons in the oldest and least peralkaline comendites (Macdonald *et al.*, 1987) points to the occurrence of this accessory phase in the magmatic system, but its stability in the more peralkaline lavas from Gorge Farm (AI 1·4) is, however, doubtful. The Zr saturation level for such peralkaline melts should be in the range of 10 000–15 000 ppm compared with <100 ppm of Zr in melts with an AI of 1·0 (Watson, 1979). Therefore, with Zr concentrations of the comendites between 1800 and 2000 ppm, crystallization and stability of zircon are impossible. Zircon, however, could be present (1) as inclusions armoured by fayalite host minerals or (2) as recent, xenocrystic zircon additions (e.g. during eruption). Given the rarity of zircon in the entire complex, this second possibility is unlikely. It is worth noting that the whole-rock data for all Gorge Farm samples of Black *et al.* (1997) define an isochron with an age of 43 ± 14 ka. These data suggest that zircon of ~46 ka age could be present in other lavas from this eruption centre. We conclude that the most plausible explanation for the extreme (^{238}U/^{232}Th) ratios of the

fayalite separates is zircons trapped as inclusions in fayalites at an early stage of the crystallization history of the comendites, i.e. when the melts were less peralkaline, as is the case for the earliest erupted comendites (Macdonald *et al.*, 1987). Consequently, the glass–fayalite ages do not reliably date the time of the last chemical fractionation of the comendites.

In summary, the internal ^{230}Th–^{238}U isochrons of the two lavas from the Gorge Farm centre (Fig. 9) are best explained by the crystallization of the accessory mineral phase chevkinite and, more speculatively, zircon armoured by fayalite host minerals. As a result of the high U and Th contents of the magma, potential fractional crystallization of chevkinite and/or zircon will not significantly change the U/Th ratios of the whole rock. Crystallization of Th-enriched chevkinite at 25 ± 10 ka and incorporation as inclusions causes a mixing relationship among the minerals in sample 504. A preceding differentiation event may have been controlled by zircon, which probably crystallized earlier during petrogenesis (47 ± 1 ka). For sample 570 these age relationships are less clear. The 50 ± 25 ka age, however, is within error of the 25 ± 10 ka age of sample 504.

Significance of Rb–Sr and U–Th age information

The combined Rb–Sr and U–Th age information for the Gorge Farm comendites indicates a major chemical fractionation event around 24 ± 1 ka that was probably related to crystallization of sanidines and a Th-enriched accessory phase (chevkinite). Unfortunately, the minor ($^{238}U/^{232}Th$) variations in the comendites only allow a resolution of ±10 ka (Fig. 9). Because of the large Rb–Sr range of the glasses, the age resolution of the Rb–Sr system (±1 ka; internal isochron) is better.

Isotopic heterogeneity (Rb–Sr–Pb) of sanidines in sample 504 and the two GF samples is related either to prolonged sanidine fractionation (until ~15 ka) or mixing–incorporation of different feldspar populations at or close to the time of eruption. Aggregation of evolving crustal melts in upper-crustal magma chambers is a possible explanation for the data, with some magma batches bringing isotopically distinct sanidine populations into the chamber where they eventually become commingled before a major period of fractional crystallization. The most significant fractionation of Rb/Sr is recorded in the Gorge Farm lavas by the 24 ± 4 ka isochron of glasses. Rb–Sr systematics of sanidine–glass pairs from comendites of the Ololbutot centre define similar ages (12 ± 4 ka) and therefore imply that this was a significant period in the thermal evolution of the Olkaria Volcanic Complex. Unfortunately, no U–Th ages could be obtained from the nearly aphyric rocks of the Ololbutot centre. The sparsely porphyritic comendites of the Olkaria complex clearly document a complex evolution and ideally require more detailed work on the phenocryst populations of the various eruptive centres.

In general, the age results from this study overlap with the age information obtained from the comprehensive work of Black *et al.* (1997), although in detail there are major differences in the measured ($^{238}U/^{232}Th$) ratios (Fig. 8). For the Gorge Farm centre, Black *et al.* (1997) reported internal isochron ages between 15 ± 2 and 36 ± 3 ka, and older ages for the Broad Acres centre (Upper Comendite Member, 50 ± 8 ka). The range of these ages resembles those obtained in this study for the Gorge Farm and for the Ololbutot centre. The lower age corresponds to the younger Rb–Sr ages of sanidine–glass pairs (Table 5) and the age of 36 ka represents the average of the U–Th ages (24 ± 10 and 50 ± 25 ka). The similarities of results are even more pronounced when taking into consideration the whole-rock data of Black *et al.* (1997), which define the earlier mentioned age of 47 ± 13 ka, similar to the glass–fayalite age of 47 ± 1 ka from this study. Nevertheless, it remains open to speculation to what extent inclusions of the accessory phases chevkinite and possibly zircon in the separates analysed by Black *et al.* (1997) are responsible for the deviating topology of their glass and whole-rock data.

Magma fractionation rates

Estimates of absolute magma fractionation rates in the Long Valley silicic magma chamber (50–800 km^3 volume) have been made using the Rb–Sr isotope system, and suggest that chemical differentiation of metaluminous rhyolitic melts operates rapidly (Halliday *et al.*, 1989; Christensen & DePaolo, 1993; Davies *et al.*, 1994; Davies & Halliday, 1998). The present study was designed to assess how the rates of magmatic processes vary with the size or composition of an igneous system. The investigated lavas of the Greater Olkaria Volcanic Complex are peralkaline rhyolites, representing ~2–10 km^3 of material erupted from spatially separated magma chambers. The results from this study lend support to models of pre-eruptive magma fractionation and thus rhyolite production in upper-crustal magma chambers, and can be utilized to infer the rates of the related processes.

Preservation of the Rb–Sr isochrons in the peralkaline rhyolites places important constraints on the physical conditions in the magma chamber. Mixing within the chamber or fractional crystallization after isochron formation would disrupt both the glass and mineral isochrons and no age information would be preserved. The fractionated magma batches of each chemostratigraphic group at Naivasha must therefore have been isolated after formation of the Rb–Sr isochron. The conclusion

of a simple sedentary magma chamber is also in contrast to other aspects of magma evolution (Davies & Macdonald, 1987; Macdonald *et al.*, 1987).

Assuming a minimum eruptive volume of $\sim 5\ km^3$ for all investigated Group 3 lava flows [deduced from the geological map of Clarke *et al.* (1990)], then the error of the Rb–Sr glass isochron (± 4 ka) indicates a magma fractionation rate of $6{\cdot}3 \times 10^{-4}\ km^3/yr$. The mineral isochron from sample 570 yields an identical age to that of the glasses but with a smaller error. These data suggest even higher magma fractionation rates ($2{\cdot}5 \times 10^{-3}\ km^3/yr$). However, determining the upper limit on fractionation rates is hampered by not knowing the actual size of the magma batch. In addition, by using the mineral isochron data one must make the assumption that the Rb–Sr systematics of the glasses from all the comendites were formed by the same, feldspar-dominated, fractionation. The glasses of the comendites have identical U–Th isotope compositions and do not provide age information on the process that produced the melts. The age resolution of the mineral U–Th isochrons is too poor to constrain magma fractionation rates, possibly because of a complex crystallization history inferred for the minor phases.

The inferred silicic magma fractionation rates are comparable with those inferred from the much larger, metaluminous, Long Valley system (up to $7{\cdot}5 \times 10^{-4}\ km^3/yr$; Davies *et al.*, 1994; Heumann & Davies, 1997; Davies & Halliday, 1998) and also argue for magma fractionation in peralkaline systems as discrete events. Importantly, however, magma storage times of ~ 25 ky for small rhyolitic systems are much shorter than those of the large Long Valley system (~ 150–250 ky; Halliday *et al.*, 1989; Reid *et al.*, 1997; Davies & Halliday, 1998). A basic compositional control (e.g. SiO_2 or alumina saturation as proxies for melt viscosity) appears too simple an explanation. More probably, the overall size of the magmatic system controls the thermal regime, degree of crystallization and the extent of thermal and compositional convection within a magma chamber. All these parameters will control the extent to which a fractionated magma can be stored in the reservoir without complete crystallization. Thus differences in crustal residence times may be best accounted for by specific parameters, such as size, longevity and thermal gradient of silicic magma systems.

CONCLUSIONS

Comendites from the Gorge Farm centre define a Rb–Sr glass isochron of 22 ± 4 ka, which is substantiated by a mineral isochron of 24 ± 1 ka. U–Th disequilibrium indicates that glasses are in secular equilibrium and have identical compositions so that no age information can be obtained. In contrast, U–Th isochrons of glasses and minerals, which yield 25 ± 10 ka and are probably controlled by the Th- and U-enriched accessory phase chevkinite, appear to confirm the Rb–Sr age. Thus, a major fractionation event at 24 ± 1 ka, most precisely defined by the Rb–Sr isochron, appears to be substantiated by two chemically independent isotope systems. In the case of the Gorge Farm centre, the last major chemical fractionation of the comendites pre-dates the eruption by ~ 16 ky. Nevertheless, despite coherent age information, relicts of earlier magma evolution ($\sim 47 \pm 0{\cdot}2$ ka) are preserved by glass–fayalite ages and clearly demand a more detailed study of the petrology of the various comendite groups. The thermal support required to sustain near-liquidus conditions in such comparatively small magmatic reservoirs (estimated 2–10 km^3) for these time scales probably demands a heat source that could comply with a larger underlying magmatic feeding system, recorded by regional basalt volcanism, or the high thermal flux of an active rift system.

ACKNOWLEDGEMENTS

Funding for this research came from the Vrije Universiteit. Coos van Belle and Richard Smeets are thanked for their expertise and laboratory assistance. Earlier versions of the manuscript benefited greatly from detailed reading and comments by Manfred van Bergen, Jon Davidson, Tim Elliott, and Jörg Keller. We thank James Gill and Ray Macdonald for valuable, constructive journal reviews. This is NSG Contribution 20010706.

REFERENCES

Bailey, D. K. & Macdonald, R. (1975). Fluorine and chlorine in peralkaline liquids and the need for magma generation in an open system. *Mineralogical Magazine* **40**, 405–414.

Bailey, D. K. & Macdonald, R. (1987). Dry felsic liquids and carbon dioxide flux through the Kenya rift zone. In: Fitton, J. G. & Upton, B. G. J. (eds) *Alkaline Igneous Rocks Geological Society, London, Special Publications* **30**, 91–105.

Baker, B. H. & Henage, L. F. (1977). Compositional changes during crystallization of some peralkaline silicic lavas of the Kenya Rift Valley. *Journal of Volcanological and Geothermal Research* **2**, 17–28.

Bevier, M. L., Armstrong, R. L. & Souther, J. G. (1979). Miocene peralkaline volcanism in west–central British Columbia—its temporal and plate tectonic setting. *Geology* **7**, 389–392.

Black, S., Macdonald, R. & Kelly, M. R. (1997). Crustal origin for peralkaline rhyolites from Kenya: evidence from U-series disequilibria and Th-isotopes. *Journal of Petrology* **38**, 277–297.

Bohrson, W. A. & Reid, M. R. (1998). Genesis of evolved ocean island magmas by deep- and shallow-level basement recycling, Socorro Island, Mexico: constraints from Th and other isotope signatures. *Journal of Petrology* **39**, 995–1008.

Bone, B. D. (1987). The geological evolution of the S.W. Naivasha volcanic complex, Kenya. Ph.D. thesis, University of Lancaster.

Bourdon, B., Zindler, A. & Wörner, G. (1994). Evolution of the Laacher See magma chamber: evidence from SIMS and TIMS measurements of U–Th disequilibria in minerals and glasses. *Earth and Planetary Science Letters* **126**, 75–90.

Caroff, M., Maury, R. C., Leterrier, J., Joron, J. L., Cotten, J. & Guille, G. (1993). Trace element behavior in the alkali basalt–comenditic trachyte series from Mururoa Atoll, French Polynesia. *Lithos* **30**, 1–22.

Christensen, J. N. & DePaolo, D. J. (1993). Time scales of large volume silicic magma systems: Sr isotopic systematics of phenocrysts in glass from the Bishop Tuff, Long Valley, California. *Contributions to Mineralogy and Petrology* **113**, 100–114.

Civetta, L., Cornette, Y., Crisci, G., Gillot, P. Y., Orsi, G. & Requejos, C. S. (1984). Geology, geochronology and chemical evolution of the island of Pantelleria. *Geological Magazine* **121**, 541–668.

Civetta, L., D'Antonio, M., Orsi, G. & Tilton, G. R. (1998). The geochemistry of volcanic rocks from Pantelleria island, Sicily channel: petrogenesis and characteristics of the mantle source region. *Journal of Petrology* **39**, 1453–1491.

Clarke, M. C. G., Woodhall, D. G., Allen, D. & Darling, G. (1990). Geological, volcanological and hydrogeological controls on the occurrence of geothermal activity in the area surrounding Lake Naivasha, Kenya. Report. Nairobi: Ministry of Energy.

Davies, G. R. & Halliday, A. N. (1998). Development of the Long Valley rhyolitic magma system: strontium and neodymium isotope evidence from glasses and individual phenocrysts. *Geochimica et Cosmochimica Acta* **62**, 3561–3574.

Davies, G. R. & Macdonald, R. (1987). Crustal influences in the petrogenesis of the Naivasha basalt–comendite complex: combined trace element and Sr–Nd–Pb isotope constraints. *Journal of Petrology* **28**, 1009–1031.

Davies, G. R., Halliday, A. N., Mahood, G. A. & Hall, C. M. (1994). Isotopic constraints on the production rates, crystallization histories and residence times of pre-caldera silicic magmas, Long Valley, California. *Earth and Planetary Science Letters* **125**, 17–37.

Drexler, J. W., Bornhorst, T. J. & Noble, D. C. (1983). Trace-element sanidine/glass distribution coefficients for peralkaline silicic rocks and their implications to peralkaline petrogenesis. *Lithos* **16**, 265–271.

Fiebig, J., Wiechert, U., Rumble, D., III & Hoefs, J. (1999). High-precision *in situ* oxygen analysis of quartz using an ArF laser. *Geochimica et Cosmochimica Acta* **63**, 687–702.

Fitton, J. G. & Upton, B. G. J. (eds) (1987). *Alkaline Igneous Rocks. Geological Society, London, Special Publications* **30**, 568 pp.

Flynn, R. T. & Burnham, C. W. (1978). An experimental determination of rare earth partition coefficients between chloride containing vapor phase and silicate melts. *Geochimica et Cosmochimica Acta* **42**, 685–701.

Fruijtier, C., Elliott, T. & Schlager, W. (2000). Mass-spectrometric ^{234}U–^{230}Th ages from the Key Largo Formation, Florida Keys, United States: constraints on diagenetic age disturbance. *Geological Society of America Bulletin* **112**, 267–277.

Gill, J. B. (1993). Melts and metasomatic fluids: evidence from U-series disequilibria and Th isotopes. *Philosophical Transactions of the Royal Society of London* **342**, 79–90.

Gill, J. B. & Williams, R. W. (1990). Th isotope and U-series studies of subduction-related volcanic rocks. *Geochimica et Cosmochimica Acta* **54**, 1427–1442.

Green, T. H. & Pearson, N. J. (1988). Experimental crystallization of chevkinite/perrierite from REE-enriched silicate liquids at high pressure and temperature. *Mineralogical Magazine* **52**, 113–120.

Halliday, A. N., Mahood, G., Holden, P., Metz, J. M., Dempster, T. J. & Davidson, J. P. (1989). Evidence for long residence times of rhyolite magma in the Long Valley magma system; the isotopic record in the precaldera rhyolite lavas of Glass Mountain. *Earth and Planetary Science Letters* **94**, 274–290.

Halliday, A. N., Davidson, J. P., Hildreth, W. & Holden, P. (1991). Modelling the petrogenesis of high Rb/Sr silicic magmas. *Chemical Geology* **92**, 107–114.

Heumann, A. (1999). Timescales of processes within silicic magma chambers. Ph.D. thesis, Vrije Universiteit Amsterdam.

Heumann, A. & Davies, G. R. (1997). Isotopic and chemical evolution of the post-caldera rhyolitic system at Long Valley, California. *Journal of Petrology* **38**, 1661–1678.

Heumann, A., Davies, G. R. & Elliott, T. (2002). Crystallisation history of rhyolites at Long Valley, California, inferred from combined U-series and Rb–Sr isotope systematics. *Geochimica et Cosmochimica Acta* (in press).

Keppler, H. (1993). Influence of fluorine on the enrichment of high field strength trace elements in granitic rocks. *Contributions to Mineralogy and Petrology* **114**, 479–488.

Knesel, K. M., Davidson, J. P. & Duffield, W. A. (1999). Evolution of silicic magma through assimilation and subsequent recharge: evidence from Sr isotopes in sanidine phenocrysts, Taylor Creek Rhyolites, NM. *Journal of Petrology* **40**, 773–786.

Lowenstern, J. B. & Mahood, G. A. (1991). New data on magmatic H_2O contents of pantellerite with implications for petrogenesis and eruptive dynamics at Pantelleria. *Bulletin of Volcanology* **54**, 78–83.

Macdonald, R. (1987). Quaternary peralkaline silicic rocks and caldera volcanoes of Kenya. In: Fitton, J. G. & Upton, B. G. J. (ed.) *Alkaline Igneous Rocks. Geological Society, London, Special Publications* **30**, 313–333.

Macdonald, R., Davies, G. R., Bliss, C. M., Leat, P. T., Bailey, D. K. & Smith, R. L. (1987). Geochemistry of high-silica peralkaline rhyolites, Naivasha, Kenya Rift Valley. *Journal of Petrology* **28**, 979–1008.

Macdonald, R., Navarro, J. M., Upton, B. G. J. & Davies, G. R. (1994*a*). Strong compositional zonation in peralkaline magma: Menengai, Kenya Rift Valley. *Journal of Volcanological and Geothermal Research* **60**, 301–325.

Macdonald, R., Williams, L. A. J. & Gass, I. G. (1994*b*). Tectonomagmatic evolution of the Kenya rift valley: some geological perspectives. *Journal of the Geological Society, London* **151**, 879–888.

Mahood, G. A. (1981). Chemical evolution of a late Pleistocene rhyolitic center. Sierra La Primavera, Jalisco, Mexico. *Contributions to Mineralogy and Petrology* **77**, 129–149.

Mahood, G. A. (1984). Pyroclastic rocks and calderas associated with strongly peralkaline magmatism. *Journal of Geophysical Research* **89**, 8540–8552.

Mahood, G. A. & Stimac, J. A. (1990). Trace-element partitioning in pantellerites and trachytes. *Geochimica et Cosmochimica Acta* **54**, 2257–2276.

Marshall, A. S., Hinton, R. W. & Macdonald, R. (1998). Phenocryst fluorite in peralkaline rhyolites, Olkaria, Kenya Rift Valley. *Mineralogical Magazine* **62**, 477–486.

McIntyre, G. A., Brooks, C., Compston, W. & Turek, A. (1966). The statistical assessment of Rb–Sr isochrons. *Journal of Geophysical Research* **71**, 5459–5468.

Michael, P. J. (1983). Chemical differentiation of the Bishop tuff and other high-silica magmas through crystallization processes: reply. *Geology* **11**, 623–624.

Mooney, W. D. & Christensen, N. I. (1994). Composition of the crust beneath the Kenya Rift. *Tectonophysics* **236**, 391–408.

Mungall, J. E. & Martin, R. F. (1995). Petrogenesis of basalt–comendite and basalt–pantellerite suites, Terceira, Azores, and some implications for the origin of ocean-island rhyolites. *Contributions to Mineralogy and Petrology* **119**, 43–55.

Nelson, S. A. & Hegre, J. A. (1990). Volcàn Las Navajas, a Pliocene–Pleistocene trachyte–peralkaline rhyolite volcano in the northwestern Mexican volcanic belt. *Bulletin of Volcanology* **52**, 186–204.

Norry, M. J., Truckle, P. H., Lippard, S. J., Hawkesworth, C. J., Weaver, S. D. & Marriner, G. F. (1980). Isotopic and trace element evidence from lavas, bearing on mantle heterogeneity beneath Kenya. In: Bailey, D. K., Tarney, J. & Dunham, K. (eds) *The Evidence for Chemical Heterogeneity in the Earth's Mantle*. London: Royal Society of London, pp. 259–271.

Peiffert, C., Nguyen-Trung, C. & Cuney, M. (1996). Uranium in granitic magmas: Part 2. Experimental determination of uranium solubility and fluid–melt partition coefficients in the uranium oxide–haplogranite–H_2O–NaX (X = Cl, F) system at 770°C, 2 kbar. *Geochimica et Cosmochimica Acta* **60**, 1515–1529.

Reid, M. R., Coath, C. D., Harrison, T. M. & McKeegan, K. D. (1997). Prolonged residence times for the youngest rhyolites associated with Long Valley Caldera: ^{230}Th–^{238}U ion microprobe dating of young zircons. *Earth and Planetary Science Letters* **150**, 27–39.

Smith, M. (1994). Stratigraphic and structural constraints on mechanisms of active rifting in the Gregory Rift, Kenya. *Tectonophysics* **236**, 3–22.

Smith, M. & Mosley, P. (1993). Crustal heterogeneity and basement influence on the development of the Kenya Rift, east Africa. *Tectonics* **12**, 591–606.

Titterington, D. M. & Halliday, A. N. (1979). On the fitting of parallel isochrons and the method of maximum likelihood. *Chemical Geology* **26**, 183–195.

Verplanck, P. L., Farmer, G. L., McCurry, M. & Mertzman, S. A. (1999). The chemical and isotopic differentiation of an epizonal magma body: Organ Needle Pluton, New Mexico. *Journal of Petrology* **40**, 653–678.

Watson, E. B. (1979). Zircon saturation in felsic liquids: experimental results and applications to trace element geochemistry. *Contributions to Mineralogy and Petrology* **70**, 407–419.

Weaver, S. D., Gibson, I. L., Houghton, B. F. & Wilson, C. J. N. (1990). Mobility of rare earth and other elements during crystallization of peralkaline silicic lavas. *Journal of Volcanological and Geothermal Research* **43**, 57–70.

Webster, J. D. & Rebbert, C. R. (1998). Experimental investigation of H_2O and Cl^- solubilites in F-enriched silicate liquids; implications for volatile saturation of topaz rhyolite magmas. *Contributions to Mineralogy and Petrology* **132**, 198–207.

Wiechert, U. & Hoefs, J. (1995). An excimer laser-based micro analytical preparation technique for *in-situ* oxygen isotope analysis of silicate and oxide minerals. *Geochimica et Cosmochimica Acta* **59**, 4093–4101.

Wilding, M. C., Macdonald, R., Davies, J. E. & Fallick, A. E. (1993). Volatile characteristics of peralkaline rhyolites from Kenya: an ion microprobe, infrared spectroscopic and hydrogen isotope study. *Contributions to Mineralogy and Petrology* **114**, 264–275.

Williams, L. A. J. & Macdonald, R. (1984). Late Quaternary caldera volcanoes of the Kenya Rift Valley. *Journal of Geophysical Research* **89**, 8553–8570.

Wolff, J. A. & Storey, M. (1984). Zoning in highly alkaline magma bodies. *Geological Magazine* **121**, 563–575.

York, D. (1969). Least squares fitting of a straight line with correlated errors. *Earth and Planetary Science Letters* **5**, 320–324.